Progress In Electromagnetics Research C, Vol. 86, 123–136, 2018

Diagnostic Method of Rotor Cracks and Local Demagnetization by Using the Measuring Coils for the Permanent Magnet Synchronous Machines

Flyur R. Ismagilov, Viacheslav Ye. Vavilov*, Denis V. Gusakov, Aibulat Kh. Miniyarov, and Valentina V. Ayguzina

Abstract—This paper proves that the use of conventional diagnostic methods of rotor crack and local demagnetization based on the harmonic analysis of the output voltage or counter-electromotive force is effective only with a certain ratio of the number of slots and poles. This statement was proved experimentally. The diagnostic method of the rotor cracks and local demagnetization which is universal for all types of windings and the number of slots of 2-pole synchronous electric machines with permanent magnets is proposed. The mathematical apparatus for the implementation of the proposed method is developed and verified with the help of FEM and experimental studies. All the experimental studies have been carried out for various rotor magnetic systems and a different number of stator slots.

1. INTRODUCTION

Permanent Magnet Synchronous Machines (PMSMs) have found wide application in all industries. They have low weight characteristics, a high specific torque and specific power, which makes it possible to effectively use them in transport, oil, machine tool and aerospace industries [1]. As a PMSM is non-contact, it finds a large-scale application in one of the most innovative branches of electromechanics — high-speed electromechanical systems. They are the most effective solution for creating high-speed generators with a rotational speed from 24,000 to 800,000 rpm. These generators are used in microturbine installations of autonomous power engineering, power supply systems for aircraft, space vehicles and automobiles [2]. Due to their high efficiency and controllability, they are used to create high-speed electric motors for machine tools, medical equipment and optical applications [3]. That is, PMSM is used in highly responsible systems, and therefore, it is necessary to predict and diagnose all of their faults in a real time.

One of the main and difficult faults for identification that may occur during their operation and manufacture is a partial demagnetization of the permanent magnets (PM) of the rotor PMSM or mechanical damage to the integrity of the PM, for example, the emergence of split, cracks, etc. Demagnetization of the PM can occur with a PMSM short-circuit under the influence of a shock current or in the case of PM overheating. This demagnetization can be subjected to a small portion of the PM, not the entire pole. Therefore, a partial demagnetization is very difficult to determine during operation, as it may not manifest itself in visible conditions but will lead to an increase in the current consumption of PMSM, a decrease in its efficiency, and lead to pulsations of electromagnetic and mechanical moment [4–6].

PM splits and cracks are a more difficult to determine defect of the PMSM rotor. They can occur when the PMSM rotor is being transported or installed in PMSM. Because the rotor PMs are in the

Received 2 July 2018, Accepted 6 August 2018, Scheduled 14 August 2018
* Corresponding author: Viacheslav Ye. Vavilov (s2_88@mail.ru).
The authors are with the Department of Electromechanics, Ufa State Aviation Technical University, 12 K. Marx Street, Ufa 450008, Russian Federation.

sleeve, the mechanical PM defects cannot be visually determined. In addition, the PM cracks and splits can be insignificant and have almost no effect on voltages and currents of PMSM. Mechanical loads of the rotor will lead to the further PM destruction during the PMSM operation especially in high-speed systems. This can lead to a complete or partial failure of PMSM.

Another problem with PM partial demagnetization is the difficulty in monitoring the rotor position. This problem occurs when the Hall sensors are used, which reacts directly to the magnetic system of the rotor itself.

Methods based on additional current injection are used to solve PMSM diagnostic problems [7–9]. Their disadvantage is the algorithmic complexity of implementation. Methods based on changing PMSM parameters for various malfunctions are presented in [10–13]. The drawbacks of these methods are that the PMSM parameters are also affected by the ambient temperature and its change can lead to erroneous diagnostics. In [14] diagnostic methods are considered and in addition to other criteria the angle of the rotor position is also introduced. The most effective and frequent method used in practice is harmonic analysis of the consumed voltage or counter-electromotive force (CEMF) using the Velvet conversion or Fourier transform. These methods are considered in [15–18]. Experimental studies of the effect of rotor cracks and local demagnetizations on the characteristics of the 6-slot PMSM with a 2-pole magnetic system and a tooth-coil winding were carried out. It is found that the use of conventional diagnostic methods is effective only with a certain ratio of the number of slots and poles. This conclusion is based on experimental studies of several defective and serviceable PMSM prototypes with a tooth-coil winding. The results of the studies, as well as the characteristics of the samples themselves, are given in this paper. A method for determining the rotors cracks and local demagnetization for 2-pole PMSM was proposed based on the use of an additional three-phase tooth-coil winding. According to this method, a universal system for rapid diagnostics of the rotor state of 2-pole PMSMs can be created.

For the practical implementation of the method, an analytical model is developed that describes the magnetic field in the PM rotor with cracks and local demagnetizations. The proposed analytical model is confirmed by FEM. Several experimental samples with different rotor magnet systems and numbers of stator slots are developed which confirms the effectiveness of the method and analytical model. The main contribution of this paper is to prove that the use of methods based on the harmonic analysis of the output voltage or CEMF is effective only with a certain ratio of the number of slots and poles. It means that diagnostic criteria cannot be extended from the results of one PMSM study to another one with a different number of slots and poles. In addition, a new method for PMSM diagnosing, which may be universal in the future, was proposed. These results may be useful for engineers, developers, manufacturers, and researchers of PMSM.

The paper is structured as follows. Section 2 presents experimental studies of SEMPM prototypes with a 6-slot tooth-coil winding with a 2-pole magnetic system and it is proved that the use of conventional methods is effective only with a certain ratio of the number of slots and poles. In addition, a method for SEMPM diagnosing with 6 slots and 2 poles is developed and presented in Section 2. Section 3 contains analytical expressions describing electromagnetic processes with PM partial demagnetization or mechanical destruction. In addition, results of the FEM analysis are presented in this section. Section 4 provides an experimental confirmation of this method for various PMSMs types. The results of experimental studies are compared with the results of FEM and analytical models. The conclusions give a generalization of the obtained results and recommendations for their further use.

2. EXPERIMENTAL STUDIES OF ROTOR CRACKS AND LOCAL DEMAGNETIZATION FOR THE HIGH-SPEED PMSM

One of the problems arising in the framework of the high-speed PMSM study is the task of creating a method that allows the on-line diagnostics of PM cracks or local demagnetization of the high-speed PMSM rotor under the sleeve. Industrial enterprises engaged in the production of high-speed PMSM use mainly 2-pole rotor magnetic systems in their products, and more rarely use 4-pole magnetic systems [19]. The choice of a 2-pole magnetic system is caused by the desire to minimize losses in the stator magnetic core [20, 21]. Analysis of known diagnostic methods [7–18] has shown that the most effective method is the diagnostics method by CEMF. Its advantages are the ease of implementation and the minimal impact of environmental conditions on its effectiveness. The disadvantage of this method

is an inability to analyze a stationary PMSM rotor.

To formulate diagnostic criteria, an experimental study of PMSM with parameters presented in Table 1 were carried out. In experimental studies, two 2-pole rotors with and without cracks were considered (Fig. 1). These rotors are intended for use in high-speed PMSM with a 96,000-rpm rotational speed and a 5 kW power. To ensure the possibility of visual monitoring of the rotors condition, the sleeve has been removed from them. To minimize the rotor destruction risks, experimental studies were performed at a rotational speed of 2,800 rpm.

Experimental studies were performed for a 6-slot PMSM with a tooth-coil winding. This type

Table 1. Parameters of the investigated topologies.

Parameters	Rated parameters		Experimental data	
	A topology	B topology	A topology	B topology
Rotational speed, rpm	96000	96000	2800	2800
Rms-phase voltage, V	51	51	1.5	1.5
Rms-phase current at full load, A	33.3	33.3	33.3	33.3
Number of poles	2	2	2	2
Active length, mm	50	50	50	50
Stator outer diameter, mm	50	50	50	50
Rotor sleeve thickness, mm	2	2	0	0
Number of turns in phase	20	20	20	20
Resistance of stator winding, Ohm	0.035	0.028	0.035	0.028
Number of stator slots	6	6	6	6
Winding type	Tooth-coil, all teeth wound	Tooth-coil, alternate teeth wound	Tooth-coil, all teeth wound	Tooth-coil, alternate teeth wound
Winding factor	0.5	0.5	0.5	0.5
Stator core material/ magnetic flux density, T	Amorphous magnetic material 5BDSR with a thickness of 25 µm/1.3 T			
PM material, residual magnetic flux density, T/magnetic field strength, A/m	SmCo, 1.07/756000			
PM thickness, mm	5	5	5	5

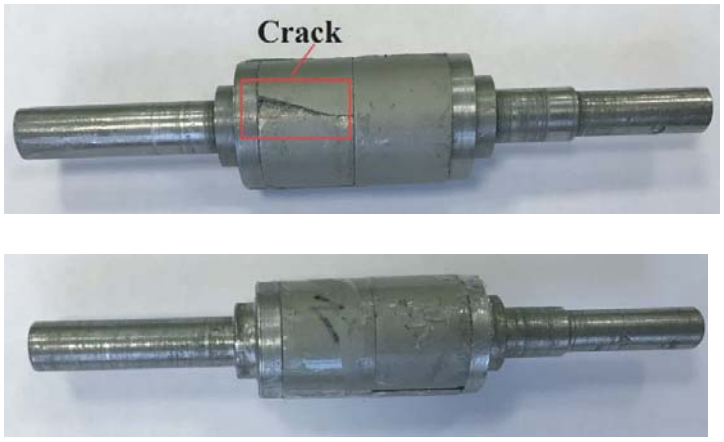

Figure 1. The investigated rotors (a) with and (b) without a crack.

of the stator magnetic core was considered since the low and medium power high-speed PMSM is technologically more efficient in the production [22]. There are 3 basic configurations of tooth-coil windings used in the industry, shown in Fig. 2. The tooth-coil winding according to Fig. 2, a (topology A, all teeth wound) has a high coefficient of use of the winding and stator core. The disadvantage of this configuration is low fault tolerance since a short circuit in one phase or in one winding can cause a short circuit in the adjacent winding or the adjacent phase. C configuration (alternate teeth wound Unequal Tooth Width) is a special case of configuration B. Its feature is the different width of the stator teeth. This configuration has development prospects for a number of applications.

Experimental studies were carried out only for topologies A and B. Topology C was not considered since it is a special case of topology of B. All the tests were performed in the generator mode when operating on an active load.

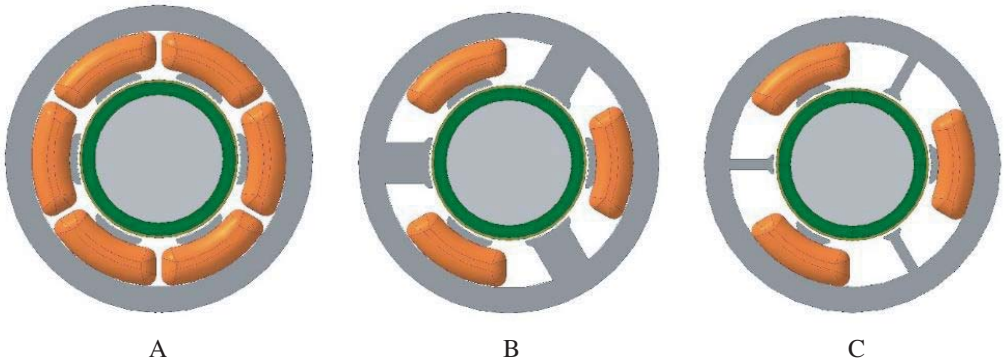

Figure 2. PMSM configurations.

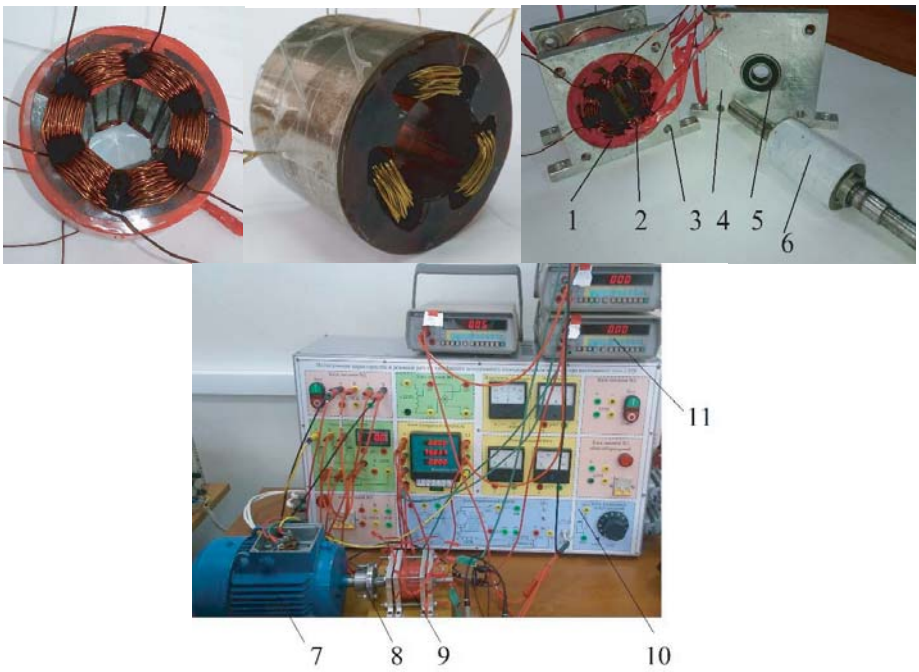

Figure 3. Experimental layout of PMSM (top) and test stand (bottom). Here: 1 is a stator magnetic core; 2 is a stator winding; 3 is a PMSM housing; 4 is a bearing shield; 5 are bearings; 6 is a rotor; 7 is a drive electric motor; 8 is a coupling; 9 is a tested layout; 10 are measuring instruments; 11 is a voltmeter.

The wire diameter was chosen as follows: the penetration depth of the magnetic field into the wire was calculated and the wire diameter was chosen to be less than this depth. The conductor for all layouts was made of two wires, each diameter being 0.8 mm. During the research, SKF 638/8-2Z bearings were used that could provide a rotational speed of up to 90,000 rpm.

Figure 3 shows the experimental layout of the 2-pole PMSM assembly. Tests of the layout were carried out on the stand; the stand is also shown in Fig. 3. The tests were performed at a lower rotational speed of 2,800 rpm. Reduced rotational speed of the rotor was used in connection with the fact that the rotor sleeve was remote. The drive motor of the stand was an asynchronous motor with a power of 4 kW.

The main task was to evaluate the EMF depending on the rotor defect. The EMF was measured with the "Gwinstek GDS-73154" oscilloscope, the harmonic voltage spectrum analysis was performed using a "Prisma-50" harmonics analyzer. The experimental results for a serviceable and defective rotor are shown in Fig. 4.

The obtained results of experimental studies of the EMF in generator mode at idle were unexpected. With the use of a defective rotor in PMSM with the tooth-coil winding type of alternate teeth wound, the output EMF becomes asymmetric with respect to the axis of the abscissas. A similar form of EMF

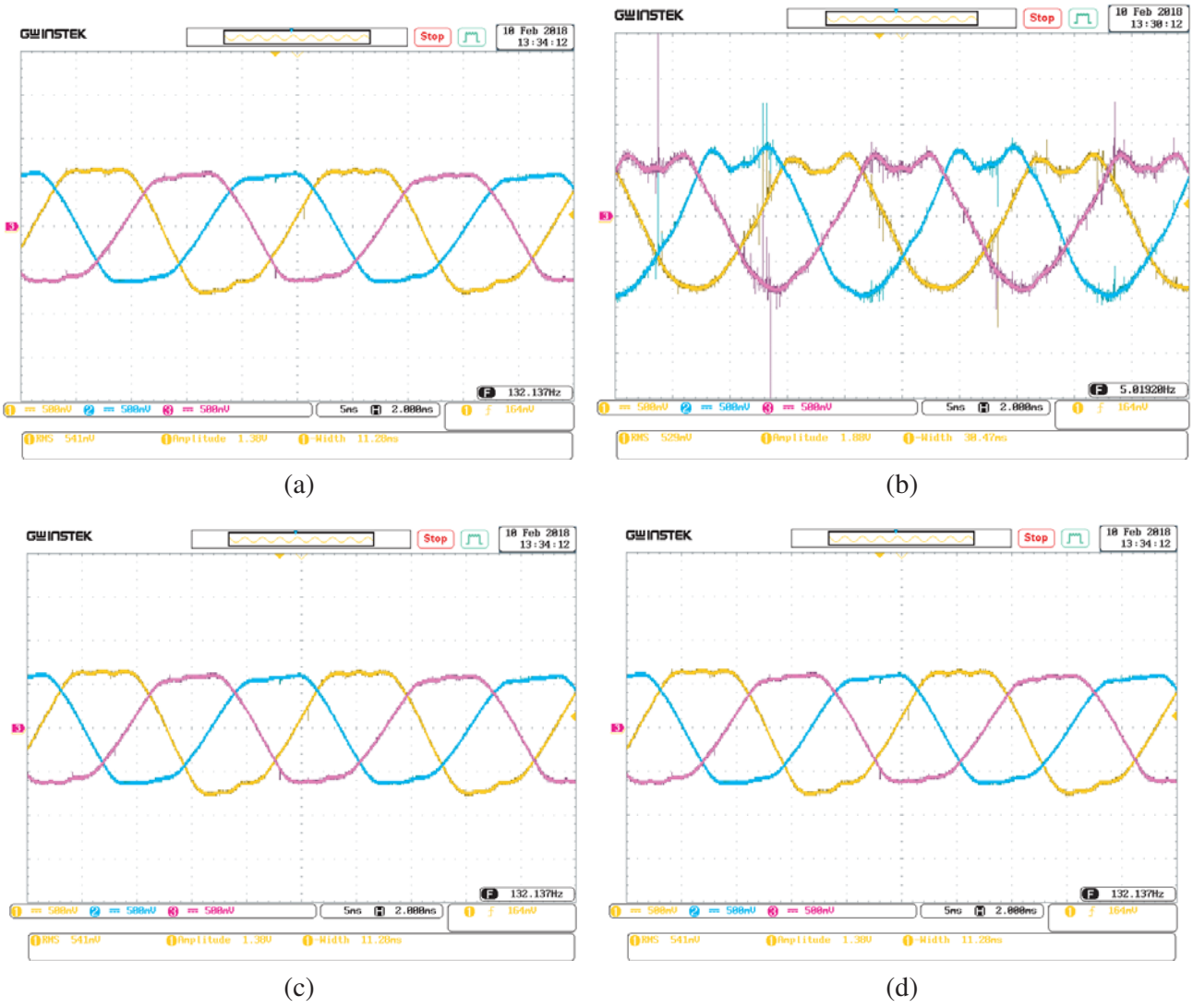

Figure 4. (a) Test results for the serviceable and (b) defective rotor of the B topology and for the (c) serviceable and (d) defective rotor of the A topology.

is practically does not occur in electric machines. The use of a serviceable rotor in this SEMPM sample resulted in the symmetry of the output EMF relative to the axis of the abscissas. Thus, the diagnostic criterion for one-side PM crack or local demagnetization for a given type of winding, number of poles and slots is the asymmetry of the output voltage along the abscissa axis. Similar results were obtained at a full load which proves that the current in the PMSM windings has practically no effect on the detected diagnostic criteria (the asymmetry of the output EMF relative to the abscissa axis).

Using the same rotors (serviceable and faulty), experimental studies were carried out on the stator magnetic core with a tooth-coil winding type of all teeth wound. The result of the experimental studies is also shown in Fig. 4. It can be seen from Fig. 4 that for a given type of windings and number of slots, the rotor defect was practically not manifested in the output EMF. This result unequivocally proves that the use of EMF as a diagnostic criterion is effective only for a certain ratio of the number of slots and poles. Diagnostic criteria cannot be extended from the study results of one PMSM to another with a different number of slots and poles.

Similar studies were also carried out for the other types of magnetic systems (magnetic systems with disk PMs and semicircular PMs, the studied magnetic systems are shown in Fig. 5), and the results were the same in all cases: for a 2-pole magnetic system in PMSM with 6 slots and a tooth-coil winding the one-sided local defect of the rotor leads to asymmetry of the output EMF. Using the same rotor for PMSM with 6 slots and a tooth-coil winding type of all teeth wound, a one-sided local rotor defect does not lead to any significant changes in the output EMF of the PMSM. The experimental results for different magnetic systems are given in the following sections.

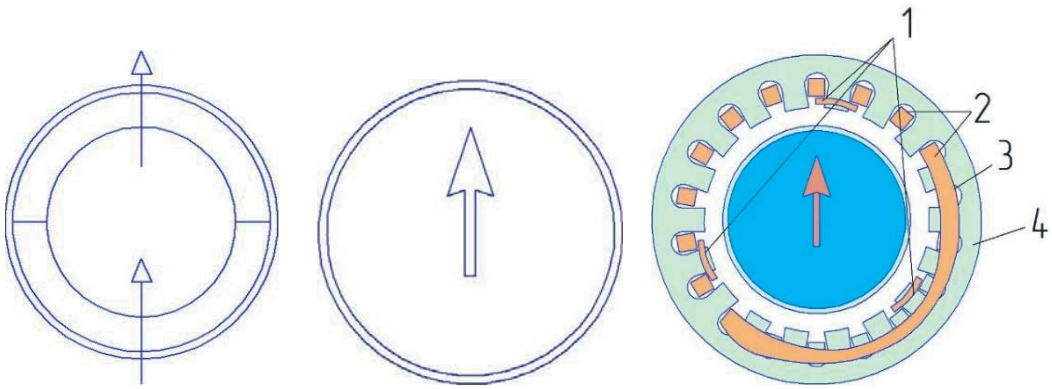

Figure 5. The studied magnetic rotor systems and an example of the location of the diagnostic winding for the 18-slot PMSM: (a) magnetic system with semicircular PM (topology A); (b) magnetic system with cylindrical PM (topology B); (c) example of laying the diagnostic winding in 18 slotted PMSM. Here: 1 is a diagnostic winding; 2 is a main winding; 3 is a frontal part of the main winding; 4 is a stator magnetic core.

A diagnostic method for the rotor crack and local demagnetization of permanent magnets for a 2-pole PMSM was proposed: to stack an additional three-phase alternating teeth wound in PMSM. This winding can have a minimum number of turns and practically do not increase the overall dimensions and weight characteristics of PMSM. The diagnostic winding should consist of three coils, each of which is a phase. In this case, the coils are located symmetrically in the three slots of the PMSM, regardless of the number of slots of the stator magnetic core. The EMF is measured from this winding and, according to the symmetry or asymmetry of this EMF, a conclusion about the technical condition of the 2-pole PMSM rotor relative to the abscissas axis is drawn. It is important to note that neither environmental conditions nor the currents induced in the PMSM windings will affect the diagnostic criteria. In addition, the proposed method does not require decomposing the output EMF in a Fourier series; its implementation requires only a comparison of several EMF values at certain points of time. The drawback of this method is that it does not allow to carry out diagnostics of PMs with a stationary rotor; and also this method is most effective at one-sided rotor local demagnetization. Studies of the

proposed method for the demagnetization of the rotor at several sites will be the tasks of next works.

The location of the windings for the method implementation using the example of an 18-slot stator is shown in Fig. 5; the rotor magnetic systems that will be studied further are also shown in Fig. 5.

Further, to study the proposed method, a mathematical apparatus was developed and computer modeling by FEM was carried out.

3. MATHEMATICAL DESCRIPTION OF THE PMSM MAGNETIC FIELD AT PM LOCAL DEMAGNETIZATION

Pole crack or local demagnetization will lead to a decrease in the magnetic flux density on the PM surface and a change in the PM magnetization amplitude. To understand the physical essence of this process, it seems reasonable to consider its mathematical description. The calculation scheme with the

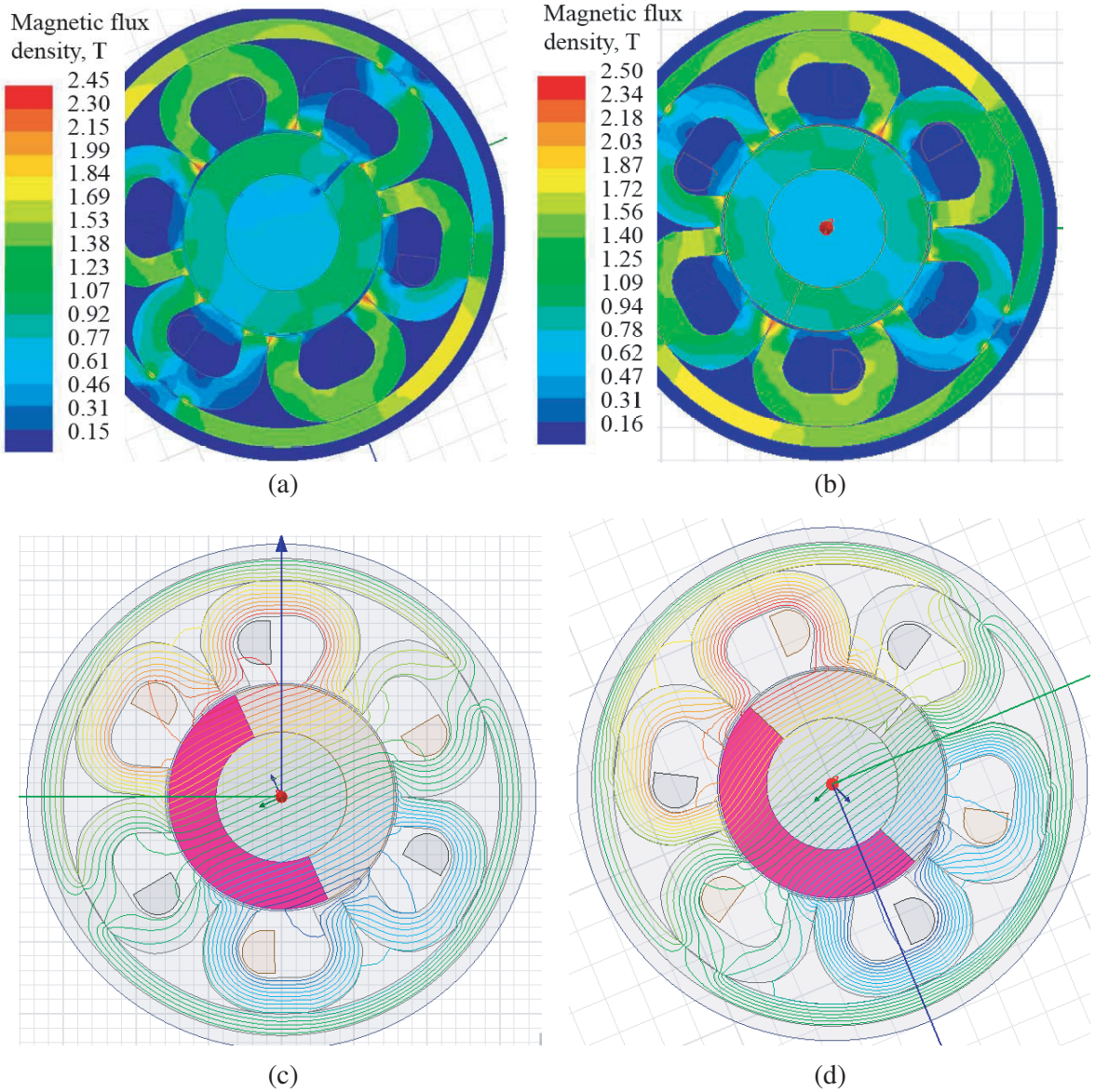

Figure 6. Distribution of magnetic flux by PMSM rotor with (a), (d) defective and (b), (c) non-defective rotors.

distribution of the magnetic flux density lines of the rotor PM is shown in Fig. 6.

In the mathematical analysis of the processes of PM local demagnetization, the following assumptions are used:

- Since the diagnostic EMF is obtained from an additional winding and is an EMF at idle, the idling magnetic field is considered;
- The 2-pole magnetic system of the rotor is considered;
- The magnetic permeability of steel core, as well as of shaft steel is equal to infinity; the magnetic permeability of the air gap is equal to the magnetic permeability of vacuum;
- The axial component of the magnetic field strength in the end surfaces of the rotor is equal to 0, i.e., PMSM of infinite length is considered;
- The winding of the PMSM being examined is presented as a thin copper layer; the current density vector contains only the axial component;
- The eddy currents induced by the space and time harmonics of the stator in PMs and the rotor sleeve are not taken into account. It is important to note here that in a number of cases, the field created by eddy currents in the windings of PMSM can also be a diagnostic criterion for crack and local demagnetization. The study of the fields of the eddy currents induced in the PMSM winding is disclosed in [24];
- The magnetic field on the surface of the PM is specified as a normal component of the harmonic series of the magnetic flux density [25]:

$$B_r(\varphi) = \sum_{n=1}^{\infty} B_{rn\max} \cos n\varphi; \quad B_{rn\max} = \frac{2}{\pi} \int_{-\frac{\pi}{2}}^{-\frac{\pi}{2}} B_M \cos^2 n\varphi d\varphi, \tag{1}$$

where $B_r(\varphi)$ is a radial component of magnetic flux density; B_M is a magnetic flux density on the PM surface; $B_{rn\max}$ is a maximum radial component of magnetic flux density.

When analyzing the magnetic field in PMSM, the Maxwell equations were used [23]:

$$\operatorname{rot}\vec{H} = \vec{j} + \vec{j}_s, \quad \operatorname{rot}\vec{E} = -\frac{\partial \vec{B}}{\partial t}, \quad \vec{j} = \sigma\left[\vec{E} + \left(\vec{V} \times \vec{B}\right)\right], \quad \operatorname{div}\vec{B} = 0, \quad \operatorname{div}\vec{j} = 0, \quad \vec{H} = \mu_0 \vec{B}, \tag{2}$$

where $\vec{B}$ is a vector of magnetic flux density of the resulting magnetic field; $\vec{E}, \vec{H}$ are the vectors of electric and magnetic field strengths, accordingly; $\vec{V}$ is a velocity vector of the rotor; σ is an electric conductivity of the stator winding; $\vec{j}$ is a density vector of induced currents; $\vec{j}_s$ is a density vector of external currents.

Since the local demagnetization of PMs should be manifested in both load modes, it is advisable to consider the PMSM idling mode for generalization of the mathematical description. To solve this problem, the Laplace equation in cylindrical coordinates was considered taking into account the continuity conditions for the lines of the magnetic field:

$$\begin{aligned} \frac{\partial^2 H_r}{\partial r^2} + \frac{1}{r}\frac{\partial H_r}{\partial r} + \frac{1}{r^2}\frac{\partial^2 H_r}{\partial \varphi^2} = 0, \\ \frac{\partial^2 H_\varphi}{\partial r^2} + \frac{1}{r}\frac{\partial H_\varphi}{\partial r} + \frac{1}{r^2}\frac{\partial^2 H_\varphi}{\partial \varphi^2} = 0, \\ \frac{1}{r}\frac{\partial H_r r}{\partial r} + \frac{1}{r}\frac{\partial H_\varphi}{\partial \varphi} = 0, \end{aligned} \tag{3}$$

where H_r, H_φ are the radial and tangential components of the magnetic field strength in the non-magnetic gap of the PMSM.

The solution of Laplace's equations is presented in a general form:

$$H_r(r, \varphi) = A(r)B(\varphi), \tag{4}$$

where $A(r)B(\varphi)$ is a Laplace product.

The boundary conditions for the solutions of Laplace's equations will be the normal component of the magnetic flux density given on the surface and also the relation $H_\varphi|_{r=\frac{D_{pm}+2\delta}{2}} = 0$, which results from the assumption of an infinite permeability of core steel.

Taking into account the boundary conditions, the solution for the tangential component of the magnetic field in the air gap PMSM is sought in the form:

$$H_\varphi = \frac{A_0}{2}\frac{R_0^{\left(\frac{D_{PM}}{2}\right)}(r)}{R_0^{\left(\frac{D_{PM}}{2}\right)}\left(\frac{D_{PM}+2\delta}{2}\right)} + \sum_{n=1}^{\infty}\frac{R_n^{\left(\frac{D_{PM}}{2}+\delta\right)}(r)}{R_n^{\left(\frac{D_{PM}}{2}+\delta\right)}\left(\frac{D_{PM}}{2}\right)}\left\{A_n\cos n\varphi + B_n\sin n\varphi\right\}, \tag{5}$$

where $r = \frac{D_{\mathrm{PM}}}{2}$ is a PM radius; D_{PM} is a PM diameter; $R_0^{\left(\frac{D_{\mathrm{PM}}}{2}\right)}(r) = \ln\frac{2r}{D_{\mathrm{PM}}}$; $R_n^{\left(\frac{D_{\mathrm{PM}}}{2}+\delta\right)}(r) = \frac{-r^{2n}+\left(\frac{D_{\mathrm{PM}}+2\delta}{2}\right)}{r^n}$; A_0, A_n, B_n are the constant components, determined from the boundary conditions.

The following designation is introduced: $\frac{D_{\mathrm{PM1}}+2\delta}{2} = R_S$, $\frac{D_{\mathrm{PM}}}{2} = R_{\mathrm{PM}}$.

With this in mind, Eq. (5) is rewritten in a smaller form:

$$H_\varphi = \frac{A_0}{2}\frac{R_0^{(R_{\mathrm{PM}})}(r)}{R_0^{(R_{\mathrm{PM}})}(R_s)} + \sum_{n=1}^{\infty}\frac{R_n^{(R_S)}(r)}{R_n^{(R_S)}(R_{\mathrm{PM}})}\left\{A_n\cos n\varphi + B_n\sin n\varphi\right\}. \tag{6}$$

At this stage, it is advisable to introduce a local demagnetization of the rotor section into the mathematical description of the PMSM magnetic field. Obviously, with a PM local demagnetization, the normal component of the magnetic field on the PM surface will drop out of the harmonic Fourier series. Then, with a local demagnetization of the PM section of the PMSM rotor, it is possible to rewrite Eq. (1) besides $\varphi = \gamma$. When $\varphi = \gamma$, magnetic flux density B_M is greater or equal to zero but smaller than for other values of the angle φ. Angle γ characterizes the PM local demagnetization coordinate. The local demagnetization of the PM along the radius was not characterized.

It follows from the boundary conditions when $r = R_s$:

$$\begin{gathered}
R_0^{(R_{\mathrm{PM}})}(r) = \ln\left(1+\frac{\delta}{D_{\mathrm{PM}}}\right), \quad R_0^{(R_{\mathrm{PM}})}(R_s) = \ln\left(1+\frac{\delta}{D_{\mathrm{PM}}}\right), \quad R_n^{(R_{\mathrm{PM}})}(r) = \frac{R_s^{2n}-R_{\mathrm{PM}}^{2n}}{R_s^n}, \\
R_n^{(R_{\mathrm{PM}})}(R_s) = \frac{R_s^{2n}-R_{\mathrm{PM}}^{2n}}{R_s^n}, \quad \frac{A_0}{2} + A_n\cos n\varphi + B_n\sin n\varphi = \sum_{n=1}^{\infty} B_{rn\max}\cos n\varphi, \\
B_{rn\max} = \frac{2}{\pi}\int_{-\frac{\pi}{2}}^{-\frac{\pi}{2}} B_M\cos^2 n\varphi d\varphi,
\end{gathered} \tag{7}$$

besides $\varphi = \gamma$. When $\varphi = \gamma$ the B_M is greater or equal to zero but smaller than for other values of the angle φ. Then:

$$A_0 = 0, \quad B_n = 0, \quad \sum_{n=1}^{\infty} A_n\cos n\varphi = \sum_{n=1}^{\infty} B_{rn\max}\cos n\varphi. \tag{8}$$

By skipping the intermediate calculations, the tangential and radial components of the magnetic flux density in the PMSM air gap are determined:

$$B_r(r,\varphi) = \sum_{n=1}^{\infty} B_{rn\max}\frac{R_{\mathrm{PM}}}{r}\frac{\left(\frac{r}{R_s}\right)^n + \left(\frac{R_s}{r}\right)^n}{\left(\frac{R_{\mathrm{PM}}}{R_s}\right)^n + \left(\frac{R_s}{R_{\mathrm{PM}}}\right)^n}\cos n\varphi, \tag{9}$$

$$B_\varphi(r,\varphi) = \sum_{n=1}^{\infty} B_{rn\max}\frac{R_{\mathrm{PM}}}{r}\frac{\left(\frac{r}{R_s}\right)^n - \left(\frac{R_s}{r}\right)^n}{\left(\frac{R_{\mathrm{PM}}}{R_s}\right)^n + \left(\frac{R_s}{R_{\mathrm{PM}}}\right)^n}\sin n\varphi, \tag{10}$$

besides $\varphi = \gamma$. When $\varphi = \gamma$, $B_{rn\max}$ is greater than or equal to zero, but smaller than that for other values of the angle φ.

Thus, taking into account the above conditions the obtained expressions allow to determine the magnetic flux density in the PMSM air gap for various PM local demagnetizations.

The proposed mathematical apparatus has a more theoretical than practical orientation. At the same time, it clearly demonstrates the processes that take place in PMSM with PM local demagnetization. Further, the mathematical apparatus is verified using FEM and experiments.

The results of the computer simulation of PMSM are presented in Fig. 7. Computer simulations used the parameters, geometric dimensions and properties of the PMSM materials presented in Table 1. Two options were also considered in computer simulation: defective and serviceable rotor. Fig. 6 shows the distribution of the magnetic flux density in the active elements of PMSM with the deflected and serviceable rotor. The mechanical crack of the PM rotor was simulated by introducing a slight air gap between the PMs. The angular coordinate of the gap was 45 degrees. Saturation of the stator magnetic core was also not taken into account in computer simulation for the evaluation of the effectiveness of the proposed analytical models.

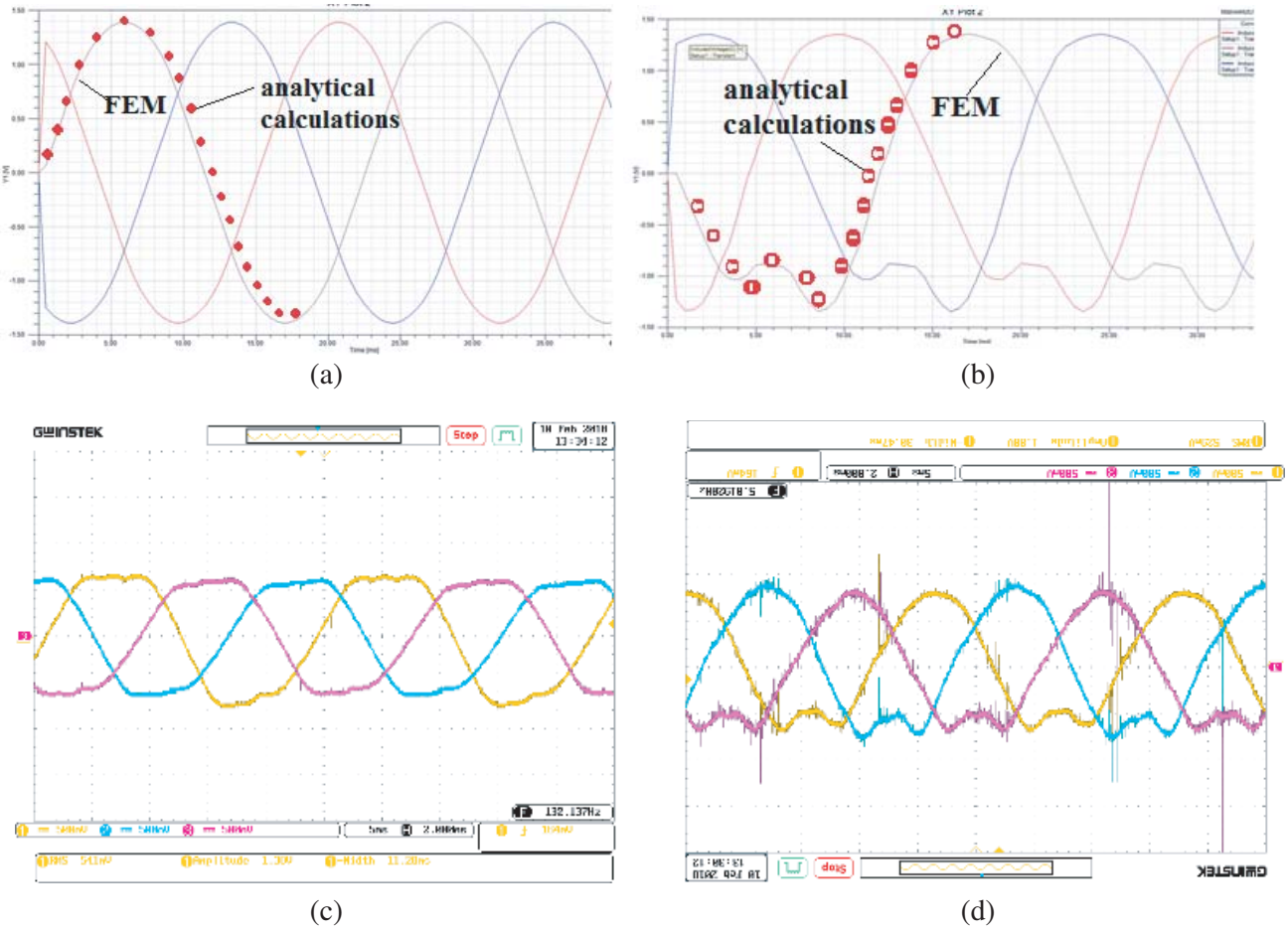

Figure 7. Comparison of analytical calculations and computer simulation with experimental results of the (a), (c) serviceable and (b), (d) defective rotor.

From the analysis of Fig. 6, it can be seen that the flux density in the active elements of PMSM is not distorted significantly. The rotor crack does not lead to an asymmetry flux density in the stator magnetic core. Therefore, mechanical crack or local demagnetization does not occur on all types of PMSM windings. In this case, the three-phase winding consisting of three coils, as can be seen from [1], is the cause of asymmetric magnetic fields. Therefore, even a non-significant asymmetry of the magnetic field is significantly reflected in its output EMF. Fig. 7 compares the results of analytical calculations

with computer simulation. From the results of comparison it is clear that the discrepancy between analytical results and FEM results is no more than 5–7%. Moreover, a comparison of the experimental results, modeling and analytical calculations with the non-defective rotor in Fig. 8 show that the shape of the output EMF curve is different. These differences are caused by the saturation of the stator magnetic core, which takes place in the experimental studies and was not considered in analytical and computer models. The numerical discrepancy between the analytical calculations, computer modeling and experimental results did not exceed 10%. This is a good result.

Figure 8. The prototype of the 18-slots PMSM with the second version of the magnetic rotor system. Here: 1 — bearing shield with bearing supports; 2, 3, 4 — lead ends of a three-phase diagnostic winding laid around one tooth; 5 — lead ends of the main power distributed winding; 6 — technological shaft; 7 — solid cylindrical rotor magnet; 8 — end shaft element.

It is important to note that both the computer simulation and analytical calculation repeated the identified diagnostic criteria. Therefore, the next research step is the experimental study of the proposed method on various ratios of the PMSM slots numbers, as well as on different magnetic systems. The results of these studies are given in Section 4.

4. EXPERIMENTAL STUDIES OF THE DIAGNOSTIC METHOD FOR PM LOCAL DEMAGNETIZATION FOR DIFFERENT ROTOR MAGNETIC SYSTEMS

To evaluate the effectiveness of the proposed diagnostic method, several experimental PMSM samples were created. The samples had a different number of slots and various rotor magnetic systems, as well as various geometric dimensions of the stator. Four types of experimental prototypes with a tooth-coil and distributed winding were investigated. Two types of rotor magnetic systems were considered, Fig. 5. The appearance of experimental rotors with a magnetic system A is shown in Fig. 1. The magnetic system B is shown in Fig. 8.

All experimental studies were performed in the generator mode at the stand shown in Fig. 3.

Table 2 and Fig. 8 show the characteristics and appearance of the prototype with the distributed winding. The prototype is shown in Fig. 3. In each of these prototypes, an inoperative rotor with a magnetic system A and B was installed and a special measuring three-phase alternating teeth wound winding was placed on the stator of each of the prototypes. The CEMF was measured from the main winding and from the diagnostic winding.

The measuring winding consisted of three coils, each of which is a phase. In this case, the coils are located symmetrically in the three slots of the PMSM, regardless of the number of slots of the stator core.

The results of experimental studies for some cases are shown in Fig. 9. The results of experimental studies for topology B are similar to those shown in Fig. 7. The results for topology D are analogous to the results of topology C. Therefore, the results for these topologies are not shown in the figures.

From the experimental results, it can be seen that there are no disturbances on the CEMF of the main winding with a faulty rotor. In this case, the EMF of the measuring winding has significant

Table 2. Characteristics of the experimental models.

Prototype	A	B	C	D
Type of rotor magnetic system	Fig. 5(a)	Fig. 5(a)	Fig. 5(b)	Fig. 5(b)
Type of stator winding	Distributed	Tooth-coil	Distributed	Tooth-coil
Number of stator slots	18	6	18	6
Rotational speed, rpm	2800	2800	2800	2800
Outer stator diameter, mm	65	60	65	60
Inner stator diameter, mm	40	32	40	32
Outer rotor diameter	25	25	28	28
Active stator length, mm	50	50	50	50

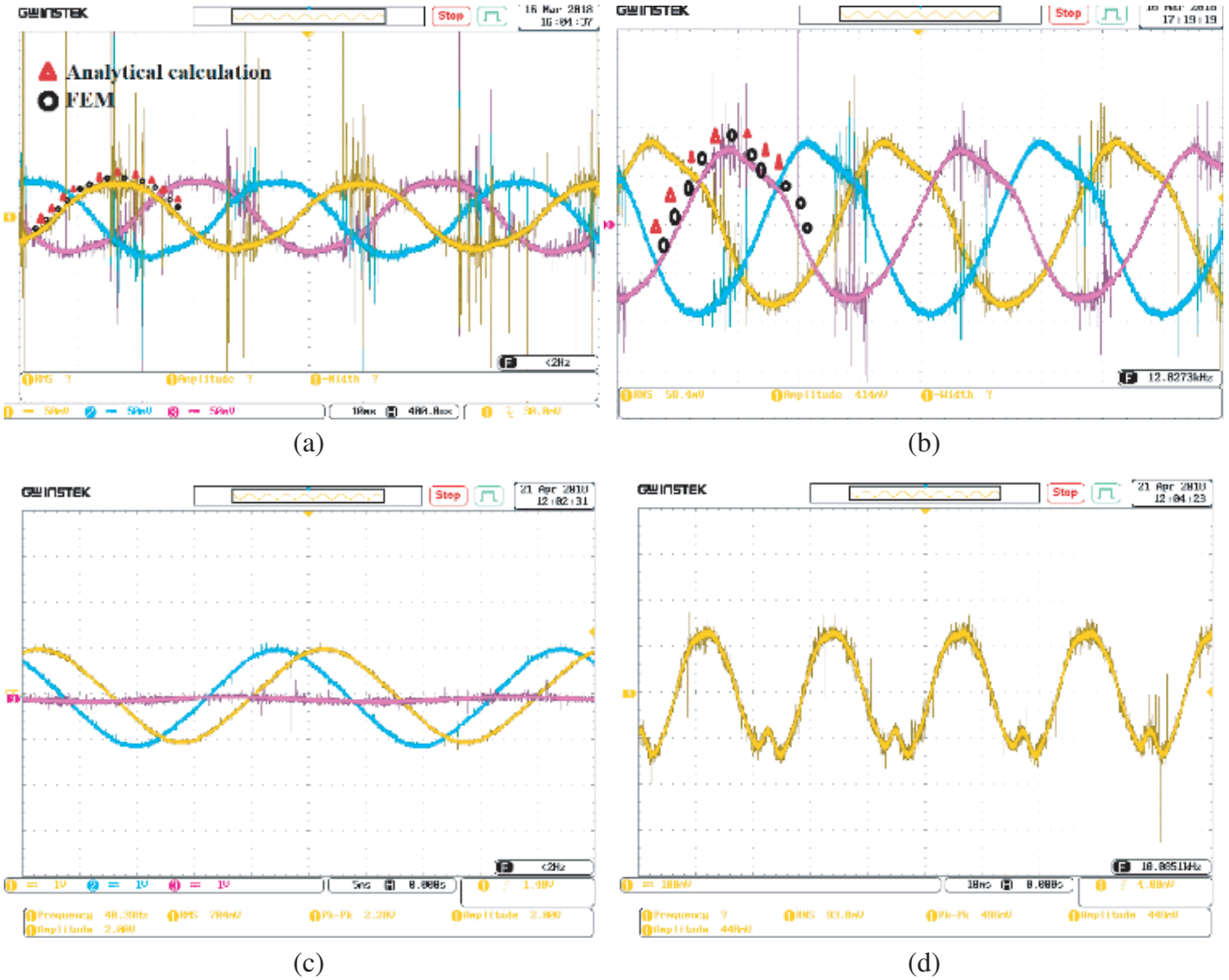

Figure 9. Results of experimental studies, (a) topology C, CEMF of the main winding; (b) topology C, CEMF of measuring winding; (c) topology D, CEMF of the main winding; (d) topology D, CEMF of measuring winding.

distortion and asymmetry relative to the abscissa axis regardless of the magnetic system type. That is, the experimental results of various geometric dimensions and parameters of PMSM unequivocally confirm the efficiency and workability of the proposed method for the diagnosis of cracks and prove the possibility of using it for all 2-pole magnetic systems and for any number of slots.

In addition, a results comparison of the proposed analytical and computer models with experimental data is presented in Fig. 9. From these comparisons it can be seen that the discrepancy does not exceed 8–10%, which makes it possible to use the developed models in practice to create an algorithmic description of the proposed diagnostic method.

5. CONCLUSION

In this paper, by conducting experimental studies of the effect of rotor cracks and local demagnetization on the characteristics of the 6-slot 2-pole PMSM with a tooth-coil winding, it was found that the use of methods based on the harmonic analysis of the output voltage or CEMF is effective only with a certain ratio of the number of slots and poles. Based on the experimental studies, the diagnostic method of the rotor cracks and local demagnetization was developed, which is universal for all types of windings and the number of slots of 2-pole PMSMs. The mathematical apparatus for the implementation of the proposed method is developed and is verified with the help of FEM and experimental studies.

It is important to note that all experimental studies have been carried out for various rotor magnetic systems and a different number of stator slots. This allowed us to unambiguously confirm the effectiveness of the proposed method.

Further research development will be the creation of an automated system for the diagnosis of PM cracks and local demagnetization of PMSMs based on the found dependencies and the developed models and the introduction of this system to industrial partners.

ACKNOWLEDGMENT

The work was supported by the Russian Science Foundation, project 17-79-20027.

REFERENCES

1. Borisavljevic, A., H. Polinder, and J. Ferreira, "On the speed limits of permanent-magnet machines," *IEEE Transactions on Industrial Electronics*, Vol. 57, No. 1, 220–227, 2010.
2. Gieras, J. F., "High speed machines," *Advancements in Electric Machines (Power Systems)*, 81–113, 2008.
3. Ganev, E., "Selecting the best electric machines for electrical power-generation systems: High-performance solutions for aerospace More electric architectures," *IEEE Electrification Magazine*, Vol. 2, No. 3, 13–22, Dec. 2014.
4. Liu, K., Q. Zhang, J. Chen, Z. Q. Zhu, and J. Zhang, "Online multi-parameter estimation of non-salient pole PM synchronous machines with temperature variation tracking," *IEEE Transactions on Industrial Electronics*, Vol. 58, No. 5, 1776–1788, May 2011.
5. Liu, K. and Z. Q. Zhu, "Online estimation of rotor flux linkage and voltage source inverter nonlinearity in permanent magnet synchronous machine drives," *IEEE Transactions on Power Electronics*, Vol. 29, No. 1, 418–427, Jan. 2014.
6. Vinson, G., M. Combacau, T. Prado, and P. Ribot, "Permanent magnets synchronous machines fault detection and identification," *IECON 2012 — 38th Annual Conference on IEEE Industrial Electronics Society*, 3925–3930, Oct. 2012.
7. Haylock, J. A., B. C. Mecrow, A. G. Jack, and D. J. Atkinson, "Operation of fault tolerant machines with winding failures," *IEEE Transactions on Energy Conversion*, Vol. 14, No. 4, 1490–1495, 1999.
8. Mecrow, B. C., A. G. Jack, J. A. Haylock, and J. Coles, "Fault-tolerant permanent magnet machine drives," *IEE Proceedings — Electric Power Applications*, Vol. 143, No. 6, 437–442, 1996.

9. Mitcham, A. J., G. Antonopoulos, and J. J. A. Cullen, "Implications of shorted turn faults in bar wound PM machines," *IEE Proceedings — Electric Power Applications*, Vol. 151, No. 6, 651–657, 2004.
10. Liu, K., Z. Q. Zhu, and D. A. Stone, "Parameter estimation for condition monitoring of PMSM stator winding and rotor permanent magnets," *IEEE Transactions on Industrial Electronics*, Vol. 60, No. 12, 5902–5913, Dec. 2013.
11. Jabbar, M. A., J. Dong, and Z. Liu, "Determination of machine parameters for internal permanent magnet synchronous motors," *Second International Conference on Power Electronics, Machines and Drives*, Vol. 2, 805–810, 2004.
12. Underwood, S. and I. Husain, "Online parameter estimation and adaptive control of permanent-magnet synchronous machines," *IEEE Transactions on Industrial Electronics*, Vol. 57, No. 7, 2435–2443, Jul. 2010.
13. Hamida, M. A., J. D. Leon, A. Glumineau, and R. Boisliveau, "An adaptive interconnected observer for sensorless control of PM synchronous motors with online parameter identification," *IEEE Transactions on Industrial Electronics*, Vol. 60, No. 2, 739–748, Feb. 2013.
14. Liu, K. and Z. Q. Zhu, "Position-offset-based parameter estimation using the adaline NN for condition monitoring of permanent-magnet synchronous machines," *IEEE Transactions on Industrial Electronics*, Vol. 62, No. 4, 2372–2383, Apr. 2015.
15. Ebrahimi, B. M., J. Faiz, and M. J. Roshtkhari, "Static-, dynamic- and mixed-eccentricity fault diagnoses in permanent-magnet synchronous motors," *IEEE Transactions on Industrial Electronics*, Vol. 56, No. 11, 4727–4739, Nov. 2009.
16. Ruiz, J. R., J. A. Rosero, A. G. Espinosa, and L. Romeral, "Detection of demagnetization faults in permanent-magnet synchronous motors under nonstationary conditions," *IEEE Transactions on Magnetics*, Vol. 45, No. 7, 2961–2969, Jul. 2009.
17. Uresty, J. C., J. R. Riba, and L. Romeral, "A back-emf based method to detect magnet failures in PMSMs," *IEEE Transactions on Magnetics*, Vol. 49, No. 1, 591–598, Jan. 2013.
18. Leboeuf, N., T. Boileau, B. Nahid-Mobarakeh, G. Clerc, and F. Meibbody Tabar, "Real-time detection of interturn faults in PM drives using back-EMF estimation and residual analysis," *IEEE Transactions on Industry Applications*, Vol. 47, No. 6, 2402–2412, Nov.–Dec. 2011.
19. Borisavljevic, A., *Limits, Modeling and Design of High-speed Permanent Magnet Machines*, 218, Springer-Verlag Berlin Heidelberg, 2013.
20. Yakupov, A. M., F. R. Ismagilov, I. H. Khayrullin, and V. E. Vavilov, "Method of designing high-speed generators for the biogas plant," *International Journal of Renewable Energy Research*, Vol. 6, No. 2, 447–454, 2016.
21. Uzhegov, N., E. Kurvinen, J. Nerg, J. T. Sopanen, and S. Shirinskii, "Multidisciplinary design process of a 6-slot 2-pole high-speed permanent-magnet synchronous machine," *IEEE Transactions on Industrial Electronics*, Vol. 63, No. 2, Feb. 2016.
22. Ismagilov, F. R., V. E. Vavilov, and R. D. Karimov, "Improving the efficiency of electrical high-RPM generators with permanent magnets and tooth winding," *Progress In Electromagnetics Research M*, Vol. 63, 93–105, 2018.
23. Ismagilov, F. R., V. Y. Vavilov, A. H. Miniyarov, A. M. Veselov, and V. V. Ayguzina, "Design, optimization and initial testing of a high-speed 5-kw permanent magnet generator for aerospace application," *Progress In Electromagnetics Research C*, Vol. 79, 225–240, 2017.
24. Ismagilov, F. R., V. E. Vavilov, D. V. Gusakov, and V. V. Ayguzina, "Eddy currents in the rotor shroud and permanent magnets of high-speed electric machines," *International Review of Aerospace Engineering*, Vol. 10, No. 6, Dec. 2017.
25. Ledovsky, A. N., *Electric Machines with High-coercivity Permanent Magnets*, 169, Energoatomizdat, Moscow, 1985.